INTERNATIONAL ATOMIC ENERGY AGENCY
UNITED NATIONS EDUCATIONAL, SCIENTIFIC AND CULTURAL ORGANIZATION

INTERNATIONAL CENTRE FOR THEORETICAL PHYSICS
34100 TRIESTE (ITALY) - P.O.B. 586 - MIRAMARE - STRADA COSTIERA 11 - TELEPHONES: 224281/2/3/4/5/6
CABLE: CENTRATOM - TELEX 460392-I

SMR/115 - 60**

WINTER COLLEGE ON LASERS, ATOMIC AND MOLECULAR PHYSICS

(21 January - 22 March 1985)

Topical Meeting on Multiphoton Processes

INFRARED MULTIPHOTON DISSOCIATION OF $^{13}CF_3Cl$

M. NEVE DE MEVERGNIES
C.E.N.
2400 Mol
Belgium

Topical Meeting on Multiphoton Processes, Miramare (Trieste), 18-22 March 1985

INFRARED MULTIPHOTON DISSOCIATION OF $^{13}CF_3Cl$

M. NEVE de MEVERGNIES
C.E.N./S.C.K., 2400 MOL, Belgium

INTRODUCTION

Multiphoton dissociation (MPD) of gaseous halomethanes induced by CO_2 laser pulses has been studied extensively in the past, among others its isotopic selectivity with respect to the carbon isotopes ^{12}C and ^{13}C. Recently, it has been proposed to apply this last property for practical separation of the carbon isotopes, using either CF_2HCl [1,2] or CF_3I or CF_3Br [3] or CF_3Cl [4] as target molecule.

Thus, besides its scientific interest, a study of the MPD of these molecules can have some practical interest.

We have previously studied the effect of gas pressure and laser pulse length on the isotopic selectivity and dissociation yield of the MPD of CF_3Cl [5,6]. The present study reports on the effect of laser pulse energy and gas pressure in a much more extended range than in our previous work.

EXPERIMENTAL

The ν_1 fundamental vibration (stretching mode) of $^{13}CF_3Cl$ occurs around 1081 cm^{-1}. Drouin et al [7] have shown that excitation of this mode can induce MPD with high isotopic selectivity and that hexafluoroethane and chloride are the only stable end products detected :

$$CF_3Cl + nh\nu \rightarrow CF_3 + Cl \rightarrow 1/2(C_2F_6 + Cl_2) \qquad (1)$$

Thermochemical data give $\Delta H(CF_3Cl \rightarrow CF_3 + Cl) = 86$ kcal/mole = 3.73 eV. All the experiments reported here were performed using the R(10) [00°1 - 02°0] ($\bar{\nu}$ = 1071.9 cm^{-1}) CO_2 laser line, i.e. within the P-branch of the ν_1 absorption band of $^{13}CF_3Cl$.

Our laser (TEA-CO_2 multimode line-tunable Lumonics Model 203) was used without N_2 in the lasing mixture and yielded pulses of about 90 ns FWHM. The 2.8 cm dia laser beam was focused with a CdTe lens (f = 76.3 cm) within a cylindrical cell of 2 cm dia., 123 cm length and 510 cm^3 total volume. The cell was made of stainless steel with NaCl windows and was connected to a quadrupole mass spectrometer through a needle valve. The main reasons for using a long focal length are to increase the dissociation yield and to allow the use of high gas pressures without optical breakdown in the focal region. The pulse energy was measured by a pyroelectric detector (Lumonics Model 20D) and was varied by insertion of neutral filters in the incident beam. The laser repetition frequency was very low (about 0.1 Hz) so as to insure reequilibrium of the gas composition in the irradiation cell between successive laser pulses.

The average energy density (or fluence) at focus ϕ_f is related to the laser pulse energy E by : $\phi_f = E/\pi\, r_o^2$ with r_o = laser beam radius at focus. In our case, $\pi r_o^2 \cong (f\theta)^2\,\pi = 0.08\ \mathrm{cm}^2$ with θ = laser beam divergence = 2.1 mrad. In Fig. 1-7, both an E-scale and a ϕ_f-scale are given, based on the above relation.

The CF_3Cl used had the natural isotopic composition (i.e. 1.10 % ^{13}C). It was bottle gas (Air Products, type HC-13, 99.9 % min quoted purity) purified by distillation. No scavenger or buffer gas was added. At the end of each irradiation, the relative reaction yield (i.e. : the ratio of the total number of C_2F_6 product molecules to the initial number of CF_3Cl molecules) was evaluated from the (119 + 120 + 121)/(104 + 105) mass-peak ratio due to the

$$({}^{12}C_2F_5^+ + {}^{12}C^{13}CF_5^+ + {}^{13}C_2F_5^+)/({}^{12}CF_3{}^{35}Cl^+ + {}^{13}CF_3{}^{35}Cl^+)$$

ions ratio, after calibration of the mass spectrometer with known C_2F_6 - CF_3Cl mixtures. As for the $^{13}C/^{12}C$ ratio in the C_2F_6 product, it was deduced from the (120/119) mass-peak ratio due to the $^{12}C^{13}CF_5^+/^{12}C_2F_F^+$ ion pair.

It is known that when the degree of dissociation of the target gas is small, the isotopic selectivity S, i.e. the ratio of the dissociation probabilities ω_{13} and ω_{12} of the $^{13}CF_3Cl$ and $^{12}CF_3Cl$ molecules, resp., is equal to the enrichment coefficient of the product molecules. In our case :

$$S = \omega_{13}/\omega_{12} \cong \frac{1}{2} \times \frac{[{}^{12}C^{13}CF_6]:[{}^{12}C_2F_6]}{[{}^{13}CF_3Cl]:[{}^{12}CF_3Cl]} \qquad (2)$$

The irradiation was stopped when the degree of CF_3Cl dissociation reached a few 10^{-3} max.

The total dissociation probability per laser pulse ω can be deduced from the relative yield of C_2F_6 and Cl_2 if there is no recombination of the primary dissociation products and if there are no other end products with significant yields. This seems to be the case here (see below). As the dissociation probabilities per laser pulse were very small ($\leq 5.10^{-4}$, see fig. 1), one has :

$$\omega \cong -\frac{1}{N}\ln\left[1 - \frac{1}{2} \times \frac{(C_2F_6)}{(CF_3Cl)}\right] \quad (N = \text{laser pulse number}) \qquad (3)$$

As for the isotopic dissociation probabilities per laser pulse ω_{12} and ω_{13} they are related to S and to the total dissociation probability ω by the relations

$$\omega = X_o\,\omega_{13} + (1 - X_o)\,\omega_{12} \qquad (4)$$

$$\omega_{13} = \omega\,[X_o + (1 - X_o)\,S^{-1}]^{-1} \qquad (5)$$

$$\omega_{12} = \omega\,[(1 - X_o) + X_o S]^{-1} \qquad (6)$$

where X_o = initial concentration of ^{13}C in CF_3Cl = 0.0110.

RESULTS

The isotopic selectivity was measured for laser pulse energies ranging from 0.5 to 2 Joules per pulse, and for initial gas pressures ranging from 0.10 to 60 Torr. The results obtained for a few selected pressures are shown on Fig. 1 and 2. Those obtained with the other gas pressures (and not shown on Fig. 1 and 2 to preserve clarity) fall between these selected ones.

The following overall trends are found :

(a) below 5 Torr pressure, S increases with laser energy; the initial rise is maximum for 0.10 and 0.25 Torr and levels off at S = 17.5 (cfr. Fig. 1, dashed line);

(b) around 5 Torr, S is about constant with laser energy (cfr. Fig. 1, full line);

(c) at 10 Torr and beyond, S decreases exponentially with laser energy (cfr. Fig. 2).

The last case corresponds to the generally expected behaviour (see refer. [8], p. 260). Our results show that selective MPD of $^{13}CF_3Cl$ under low gas pressure follows an opposite trend. Preliminary results obtained by us with selective MPD of two other minority isotopic molecules $^{13}CF_3Br$ and $^{34}SF_6$ under low pressure show a similar trend. Thus, the "expected behaviour" mentioned above might not be as general as presently assumed.

Fig. 1 and 2 also show that at low energy (i.e. $E = 0.5$ J/pulse or $\phi_f = 5$ J/cm²), S increases with pressure from a value of 10.5 for 0.10 Torr upto a maximum of 21 for 10 Torr, and decreases beyond, down to 9.5 for 60 Torr. This trend is gradually lost for increasing laser pulse energy. The behaviour at low energy agrees qualitatively without previous results [5] obtained with 0.6 J pulse energy, the quantitative difference between the two being due to the difference between laser beam geometry ($f = 6.3$ cm in [5] and $f = 76.3$ cm in the present work). The initial increase of S with pressure is due to rotational relaxation [5,6] .

The total dissociation probability ω was measured for various gas pressures. The result is shown on fig. 3. Besides its threshold character, a rather striking feature is the fact that, within the limited accuracy of our measurements, all the results seem to be scattered around a common mean value (fig. 3, dashed line), in spite of a 600-fold change in gas pressure. Thus, from a chemical point of view, the overall reaction as given very schematically by relation (1) is first-order.

The steep rise of MPD probabilities with laser pulse energy can be due to several effects. Besides true physical effects (see Ref. [8], p. 228), purely geometrical effects appear when a focused laser beam is used, due to the threshold character of the MPD phenomenon. They have been studied in detail by a number of authors. It seems that the simplifying assumption of an ideally sharp energy density threshold is acceptable for the analysis of our results, which were mostly obtained at fluences well above threshold. Herman [9] has shown that when this simplifying assumption is adopted and supposing further a Gaussian beam intensity profile and an optically-thin medium, the effective reaction volume V_{eff} (equal to the product of the observed fractional yield per pulse and the cell volume) scales-up with the laser pulse energy E as (see Model II of Ref. [9]) :

$$V_{eff} \propto \frac{4}{3}\,(n-1)^{1/2} + \frac{2}{9}\,(n-1)^{3/2} - \frac{4}{3}\arctan\,(n-1)^{1/2} = f(n) \qquad (7)$$

with $n = 2E/(\pi\, r_o^2 \times \phi_{crit})$, r_o = laser beam radius at focus and ϕ_{crit} = critical fluence such that the MPD probability is either zero or non-zero when the laser fluence is either lower or higher than ϕ_{crit}, respectively.

A value of ϕ_{crit} was chosen, corresponding to a pulse energy value E_{crit} lying 0.1 J below the low-energy limit of our measurements (i.e. the abscissa shown by the downward-pointing arrow in Fig. 3). For a Gaussian beam profile, the relation between the fluence at focus on the beam axis, $\phi(0)$, and the laser pulse energy E is given by : $\phi(0) = 2E/\pi\, r_o^2$ with, in our case, $\pi\, r_o^2 = 0.08$ cm² (see above). Thus, the numerical values for E_{crit} and ϕ_{crit} are :

$E_{crit} = 0.3$ J/pulse; $\phi_{crit} = 7.5$ J/cm²

The value at ϕ_{crit} would be lower for a non-Gaussian beam profile. The geometrical correction (7) was applied to the ω vs. E results of Fig. 3. The experimental ω values close to threshold, i.e. for $E = 0.4$ J/pulse, were used for normalization. The isotopic dissociation probabilities ω_{12} and ω_{13} were deduced, using relations (5) and (6). Fig. 4, 5 and 6 show the data plotted vs. E^{-1} or ϕ_f^{-1} on a semi-log scale, for a few selected pressures. Those for intermediate pressures, not drawn on the Fig. to preserve clarity, show intermediate overall trends.

It is seen that they fall in 3 different categories :

(a) at low pressure (Fig. 4), an exponential decrease of both ω_{12} and ω_{13} with E^{-1} is found, the decrease being steeper for ω_{13} (dashed line) than for ω_{12} (full line);

(b) for medium pressures (Fig. 5) both ω_{12} (full line) and ω_{13} (dashed line) are about constant;

(c) for higher pressures (Fig. 6), the numerical values of ω_{12} and ω_{13} decrease with pressure, and the 60 Torr data exhibit an overall decrease with E^{-1}; however, contrary to the low-pressure case (Fig. 4), the decrease is steeper for ω_{12} than for ω_{13}.

The above results are based on relation (3), i.e. on the assumption that the MPD probability can be deduced unambiguously from the C_2F_6 yield per pulse. The value of ω_{13} can also be deduced from the decrease of the ^{13}C content of the residual CHF_3 for large values of the laser pulse number N and from the S value obtained above for low values of N. The ω value can be further deduced, using relations (2) and (4). Preliminary results show qualitative agreement with the data displayed on Fig. 3.

DISCUSSION

An evaluation of the gas kinetic collision frequency of CF_3Cl yields a value of 1.4×10^7 s^{-1} Torr^{-1}. Thus the average time between mutual collisions amounts to about 700, 70 and 1 ns for 0.10, 1 and 60 Torr pressure, resp. Comparing it with the 90 ns FWHM laser pulse duration, one can assume that the low pressure (i.e. 0.10 and 0.25 Torr) MPD results shown on Fig. 1

and 4 and the high pressure (i.e. 30 and 60 Torr) ones shown on Fig. 2 and 6 are representative of the collisionless and collisionnal regimes, respectively.

In the collisionless range (Fig. 4), the exponential decrease of ω_{12} and ω_{13} with E^{-1} or ϕ_f^{-1}, i.e. an Arrhenius-type relation, has no theoretical justification. A detailed analysis of the various physical aspects of the IR MPD excitation of a molecule in the quasi-continuum region of its level scheme yields much more complex relations (see e.g. refer. [8], p. 228 and refer. herein). It can be noted, however, that thermochemical reaction rates are very well described by Arrhenius-type relations in spite of the fact that there is no rigorous theoretical justification for it. Thus, it is perhaps not surprising that IR-MPD, with its threshold character and statistical distribution of vibrationally excited molecules, can phenomenologically be described by the same formal relation as a thermochemical reaction with an activation energy and a Maxwell distribution of molecular kinetic energies.

These considerations can be more quantitatively substantiated by comparing the experimental data with the relation :
$\omega_{13} = A \exp [-\varepsilon_{thr}/(\varepsilon.q)]$, where ε_{thr} = MPD threshold energy, ε = average energy of excited $^{13}CF_3Cl$ molecules, and q = fraction of $^{13}CF_3Cl$ being excited. From our 0.10 Torr data, one obtains $q \doteq 0.1$. Expressing the energies in Joules/pulse (with $E_{thr} = 0.30$ J/p, see Fig. 3), one thus obtains :

$$\omega_{13} = A \exp [-E_{thr}/(E \times 0,1)] \doteq A \exp [-3,0/E]$$

which is in fair agreement with the fit to the 0.10 and 0.25 Torr data (see caption of Fig. 4).

In the medium-pressure range (Fig. 5), the almost constant ω_{12} and ω_{13} values ($\sim 9 \times 10^{-7}$ and 1.5×10^{-5}, resp.) are about equal to the maximum ω-values reached in the low pressure range (see Fig. 4). The most obvious explanation is full rotational relaxation, such that within the reaction volume around the laser beam focus, all the excited molecules do dissociate.

As for the collisionnal range (Fig. 6), two features should be noted. First, the magnitudes of ω_{12} and ω_{13} fall down beyond 30 Torr pressure, due to collisionnal deactivation during or immediately after the laser pulse.

Secondly, at 60 Torr pressure a decrease of ω_{12} and ω_{13} with E^{-1} or ϕ_f^{-1} sets in. Most interesting is the fact that the slope of ω_{12} is steeper than the one of ω_{13}. This might be due to the outset of secondary reactions such as the one between excited $^{13}CF_3$ radicals and cold $^{12}CF_3Cl$ molecules, i.e. (schematically) :

$$^{13}CF_3^* + {}^{12}CF_3Cl \rightarrow {}^{13}C^{12}CF_6 + Cl \qquad (8)$$

However, the trend shown on Fig. 6 should be complemented by additionnal measurements at pressures above 60 Torr, to confirm this conclusion and possibly draw more quantitative information about reaction (8).

REFERENCES

[1] A. Outhouse, P. Lawrence, M. Gauthier, P.A. Hackett,
Appl. Phys. B36, 63 (1985)

[2] A.V. Evseev, V.S. Letokhov, A.A. Puretsky,
Appl. Phys. B36, 93 (1985)

[3] O.N. Avatkov, A.B. Bakhtadze, V.Yu. Baranov, V.S. Doljikov, I.G. Gverdtsiteli,
S.A. Kazakov, V.S. Letokhov, V.D. Pismenyi, E.A. Ryabov, V.M. Vetsko,
Appl. Optics 23, 26 (1984)

[4] K. Takeuchi, R. Nakane, I. Inoue,
J. Chem. Eng. Japan, 14, 395 (1981)

[5] M. Nève de Mévergnies,
Appl. Phys. 25, 275 (1981)

[6] M. Nève de Mévergnies,
Appl. Phys. B29, 125 (1982)

[7] M. Drouin, M. Gauthier, R. Pilon, P.A. Hackett, C. Willis,
Chem. Phys. Lett. 60, 16 (1978)

[8] V.S. Letokhov, "Nonlinear Laser Chemistry",
Springer Verlag, Berlin (1983)

[9] I.P. Herman, Opt. Lett. 4, 403 (1979)

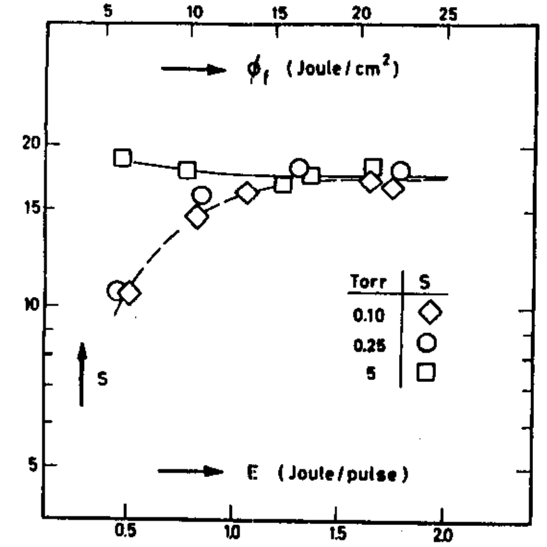

Fig. 1 : Selectivity S of the MPD of CF_3Cl vs. laser pulse energy E and average fluence in the focal plane ϕ_f, for low gas pressures.

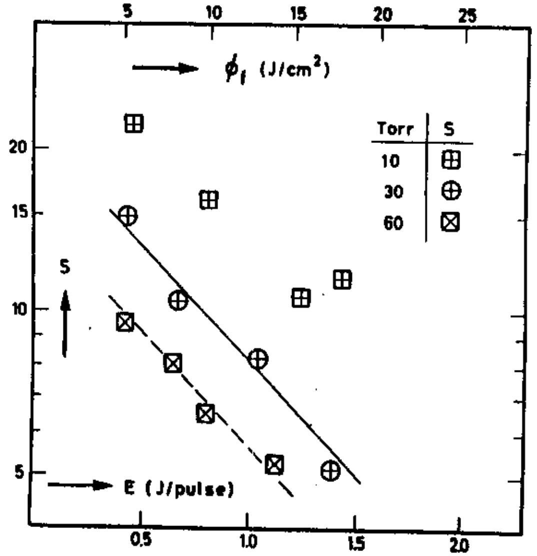

Fig. 2 : Selectivity S of the MPD of CF_3Cl vs. laser pulse energy E and average fluence in the focal plane ϕ_f, for high gas pressures.

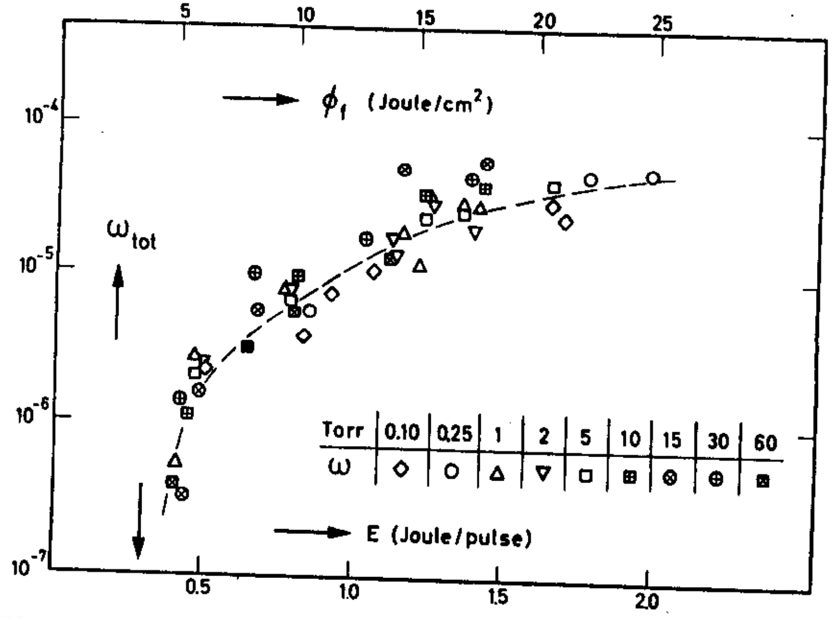

Fig. 3 : Total CF_3Cl dissociation probability per laser pulse ω_{tot} vs. E and ϕ_f for gas pressures ranging from 0.10 upto 60 Torr.

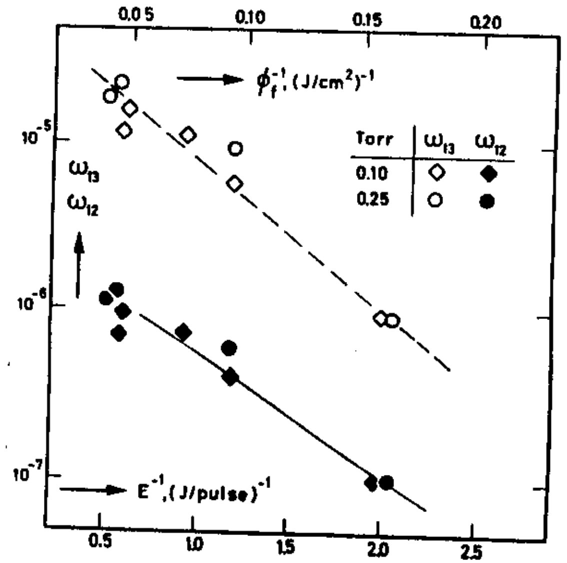

Fig. 4 : Isotopic dissociation probabilities per laser pulse , corrected for geometrical effects, vs. E^{-1} and ϕ_f^{-1}, for low gas pressures. The dashed line corresponds to $\omega_{13} = 6.2 \times 10^{-5} \times \exp(-2.06/E)$.

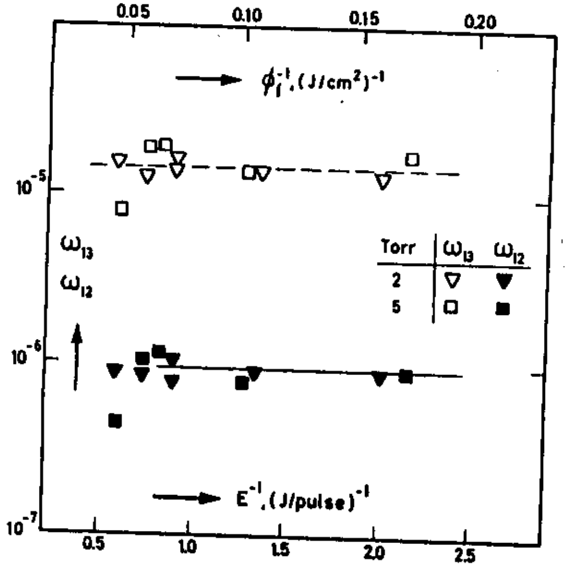

Fig. 5 : Isotopic dissociation probabilities per laser pulse, corrected for geometrical effects, vs. E^{-1} and ϕ_f^{-1}, for medium gas pressures.

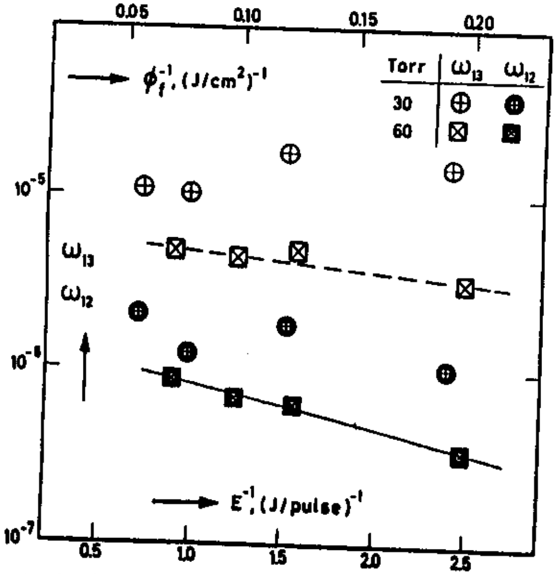

Fig. 6 : Isotopic dissociation probabilities per laser pulse, corrected for geometrical effects, vs. E^{-1} and ϕ_f^{-1}; for high gas pressures.